On the Role of Asymptomatic Carriers in Epidemic Spread Processes

Xiaoqi Bi and Carolyn L. Beck

Abstract—We present an epidemiological compartment model, SAIR(S), that explicitly captures the dynamics of asymptomatic infected individuals in an epidemic spread process. We first present a group model and then discuss networked versions. We provide an investigation of equilibria and stability properties for these models, and present simulation results illustrating the effects of asymptomatic-infected individuals on the spread of the disease. We also discuss local isolation effects on the epidemic dynamics in terms of the networked models. Finally, we provide initial parameter estimation results based on simple least-squares approaches and local test-site data.

Keywords: Epidemic dynamics, networks, data-informed modeling, stability analysis, parameter estimation

I. INTRODUCTION

Modeling, analysis and control of epidemic spread processes over networks have received increasing attention over the two past decades, owing not only to the recent COVID-19 pandemic and other viral outbreaks, but also to the plethora of computer network viruses. Conducting experiments to analyze infectious disease spread processes and response policies are prohibitive for many reasons, and effectively impossible over large human contact networks. As a result, mathematical modeling and simulation, informed by up-to-date data, provides an essential alternative for estimating and predicting when and how an epidemic will spread over a network. Moreover, simulations of strategic control policies over validated epidemic models can provide insights into approaches for mitigating spread.

Mathematical models for epidemics, or spread processes, have been proposed, analyzed and studied for over 200 years [1]. Models used for most studies today derive from the so-called *compartment models* proposed by Kermack and McKendrick in 1932 [2]. These models assume every subject lies in some segment or compartment of the population at any given time, with these compartments possibly including *susceptible* (S), *infected* (I), *exposed* (E) and/or *recovered* (R) groups, leading to the classical epidemiological models: SI, SIS, SIR and SEIR models; e.g., the SIS model is

$$\dot{S}(t) = -\beta S(t)I(t) + \delta I(t)
\dot{I}(t) = \beta S(t)I(t) - \delta I(t),$$
(1)

where S(t), I(t), resp., are the susceptible (healthy) and infected segment of the population, β represents the rate of infection or contact amongst infected and susceptible subgroups, and δ represents the healing or curing rate. This model assumes: (1) a homogeneous population with no vital dynamics (birth and death processes), implying infection and healing are assumed to occur at faster rates than with

Xiaoqi Bi and Carolyn L. Beck are with the Coordinated science Laboratory and the ISE Department, University of Illinois at Urbana-Champaign, Urbana, IL 61801, Emails: {xiaoqib2|beck3}@illinois.edu

vital dynamics and the population size remains constant; and (2) the population mixes over a trivial network, i.e., over a complete graph structure. These assumptions have led to errors in previous epidemic forecasts [3].

We note that similar models to that given in (1) have been derived for SI, SIR(S) and SEIR(S) processes; SI models simply have $\delta = 0$; SIR(S) models include a recovered segment of the population and a recovery parameter and SEIR(S) models include an exposed segment of the population, which is assumed to be non-infectious, and a corresponding parameter that captures the transition rate from the exposed state to the infected state, effectively capturing the disease incubation period. There are numerous variants of these models, including recent models in which human awareness is taken into account [4], [5], [6], [7], and in which multiple epidemic processes may be propagating simultaneously [8], [9], [10].

Over the past two decades, to address discrepancies found in prior epidemic forecasts and to better model spreading processes of computer viruses over communication networks, there has been extensive work on epidemic processes evolving over complex network structures; see for example [11], [12], [13], [14], and from a controls perspective [15]. To account for network structure, an agent-based perspective of epidemic processes is taken where each agent (an individual or subgroup in the population) is represented by a node, and the edges in the network between nodes represent the strength of the interaction between agents. Given a total of nnodes, epidemic processes can be described by large Markov process models (e.g., of dimension 2^n for SIS models and 3^n for SIR models), which capture the probability of each node transitioning from susceptible to infected, and/or to recovered states, and back. These probabilities are determined by the infection rate(s), healing rate(s) and/or recovery rate(s), and the network interconnection structure, and capture the stochastic evolution of such epidemic processes. These models become intractable to analyze as the number of nodes, n, increases; once n is large enough mean-field approximation (MFA) models become appropriate. MFA models are derived by taking expectations over infection transition rates of agents, and rely on the results of Feller [16] and Kurtz [17].

For agents interconnected via a graph with adjacency matrix $W = [W_{ij}]$, where W_{ij} represents the strength of connection from node i to node j, under the previous assumptions along with additional independence assumptions, deterministic networked MFA models are now widely applied (see

¹The literature in this area is vast, thus we cannot provide an overview of all prior research due to space constraints. However, we note that the cited papers provide extensive summaries of existing results.

[18], [19] for analysis, discussions and perspectives). Again using an SIS process example, if we denote the probability of node i being infected at time t by $p_i(t) \in [0,1]$, the following differential equation provides a MFA model for the probability of infection of node i:

$$\dot{p}_i(t) = (1 - p_i(t))\beta \sum_{j=1}^{N} W_{ij} p_j(t) - \delta p_i(t).$$
 (2)

This model provides a lower complexity deterministic approximation to the full dimension Markov process model of a SIS spread process evolving over a static network [15], [20], [21]. Discrete time versions of these approximation models have also been proposed and studied [22], [23]. Primary goals in most analyses of epidemic process dynamics include computing the system equilibria, and determining the convergence behavior of these processes near the equilibria. Specifically, conditions for the existence of and convergence to "disease-free" or "endemic" equilibria are sought.

In this paper we consider a compartment model structure that specifically accounts for *infectious but asymptomatic* subgroups or individuals, namely a SAIR(S) model structure, incorporating Susceptible (S), Asymptomatic-infected (A), Infected-symptomatic (I), and Recovered (R) subsets of the population. We note the asymptomatic subset we consider may include those individuals who do not experience symptoms through the course of their infection, as well as presymptomatic individuals. This structure may be used to directly capture the dynamics of COVID-19 and the role asymptomatic individuals play in the disease spread.²

In Section II, we present our SAIR(S) group and networked models and discuss their equilibria and stability properties. We present a series of simulation studies in Section III that illustrate our stability results as well as highlighting the role the asymptomatic subgroup plays in disease spread under various quarantine policies. In Section IV we apply a simple least squares estimation approach to compute the SAIR(S) model parameters from data, using local data (Champaign County Public Health District) for initial estimations. We note the challenges that currently available data present and our ongoing work in Section V.

II. THE SAIRS MODEL

In order to investigate the effects of asymptomatic individuals on the spread of the epidemic, we consider the fraction and effect of asymptomatic carriers directly. We evaluate both single group models as well as networked models.

A. Single-Group and Networked Models

Let S(t), A(t), I(t), R(t), resp., represent the proportion of susceptible, asymptomatic-infected, symptomatic-infected, and recovered individuals at time t. Our Group SAIR(S) model is characterized as:

²This model was first introduced in online seminars and panel discussions [24], [25], and in the literature in [26]. Compartment models with different structures but including explicit asymptomatic population segments were previously proposed for dengue fever [27] and rumor spreading over online social networks [28].

$$\dot{S}(t) = -\beta S(t)(A(t) + I(t)) + \delta R(t)
\dot{A}(t) = q\beta S(t)(A(t) + I(t)) - \sigma A(t) - \kappa A(t)
\dot{I}(t) = (1 - q)\beta S(t)(A(t) + I(t)) + \sigma A(t) - \gamma I(t)
\dot{R}(t) = \kappa A(t) + \gamma I(t) - \delta R(t)$$
(3)

Here β is the transmission rate amongst susceptible and infected groups, which includes both asymptomatic and symptomatic; κ and γ , resp., are the recovery rates for asymptomatic and symptomatic-infected groups. Additionally, q captures the proportion of individuals who are asymptomatic (and/or pre-symptomatic) but still infectious; correspondingly, (1-q) represents the proportion of symptomatic individuals. Further, σ is the progression rate from asymptomatic to symptomatic, and δ represents the rate at which immunity recedes; when $\delta=0$, individuals gain permanent immunity to the infection upon recovery. We assume these relations hold for all $t\geq 0$.

We also study the SAIR(S) model dynamics of nsubpopulations interconnected over an arbitrary network structure, with adjacency matrix denoted by W. Define s_i, a_i, p_i, r_i , resp., as the proportion of the subpopulation i that is susceptible (or healthy), asymptomaticinfected, symptomatic-infected, or recovered. The Networked SAIR(S) model (N-SAIR(S)) capturing the spread process over an arbitrary interconnection network is given by:

$$\begin{split} \dot{s}_{i}(t) &= -\beta_{i}s_{i}(t)\sum_{j}W_{ij}(a_{j}(t) + p_{j}(t)) + \delta_{i}r_{i}(t) \\ \dot{a}_{i}(t) &= q\beta_{i}s_{i}(t)\sum_{j}W_{ij}(a_{j}(t) + p_{j}(t)) - \sigma_{i}a_{i}(t) - \kappa_{i}a_{i}(t) \\ \dot{p}_{i}(t) &= (1 - q)\beta_{i}s_{i}(t)\sum_{j}W_{ij}(a_{j}(t) + p_{j}(t)) + \sigma_{i}a_{i}(t) - \gamma_{i}p_{i}(t) \\ \dot{r}_{i}(t) &= \kappa_{i}a_{i}(t) + \gamma_{i}p_{i}(t) - \delta_{i}r_{i}(t) \end{split}$$

where for a subpopulation i, the parameters β_i , κ_i , γ_i , σ_i and δ_i are defined as for the Group model. Since all individuals in a subgroup i will reside in one of these subsets, we have $s_i(t) + a_i(t) + p_i(t) + r_i(t) = 1$, over all i, j and relative to the population size, N_i of group i.

Remark: The Group Model (3) can be viewed as the Networked Model (4) in the case where we have homogeneous spread parameters and the underlying network topology is complete with evenly distributed interconnection weights; that is, when $W_{ij} = 1/n$ for all $i, j \in [n]$, and $(\beta_i, \kappa_i, \gamma_i, \sigma_i, \delta_i) = (\beta, \kappa, \gamma, \sigma, \delta)$ for all $i \in [n]$.

Prior to discussing analysis of equilibria and stability for these models, we note the following result which establishes that the N-SAIR(S) model is well-defined. This result was first presented in [26] for the discrete-time case using an induction argument; it is straightforward to adapt to the continuous-time model given in (4).

Assumption 1: For all $i \in [n]$, $\beta_i, \gamma_i, \delta_i, \kappa_i, \sigma_i$ and $W_{ij} \ge 0$ Lemma 1: Consider the model in (4) under Assumption 1. Suppose $s_i(0), a_i(0), p_i(0), r_i(0) \in [0, 1], s_i(0) + a_i(0) + p_i(0) + r_i(0) = 1$ for all $i \in [n]$. Then, for all $t \ge 0$ and $i \in [n]$, we have $s_i(t), a_i(t), p_i(t), r_i(t) \in [0, 1]$ and $s_i(t) + a_i(t) + p_i(t) + r_i(t) = 1$.

B. Equilibria and stability

To quantitatively and qualitatively evaluate the propagation of the virus, the basic reproduction number, R_0 , is a critical threshold quantity used widely in epidemiological studies. This number indicates how rapidly infected individuals transmit the virus to healthy individuals. In order to stop the virus from spreading exponentially, we require $R_0 < 1$. In this section, we evaluate the SAIR(S) system equilibria and conduct stability analysis around the equilibria, allowing us to determine a stabilizing R_0 threshold.

1) Group Model SAIRS: Noting that S(t) = 1 - A(t) - I(t) - R(t), the nonlinear system (3) can be written as:

$$\dot{A}(t) = q\beta(1 - A(t) - I(t) - R(t))(A(t) + I(t)) - \sigma A(t) - \kappa A(t)
\dot{I}(t) = (1 - q)\beta(1 - A(t) - I(t) - R(t))(A(t) + I(t)) + \sigma A(t) - \gamma I(t)
\dot{R}(t) = \kappa A(t) + \gamma I(t) - \delta R(t)$$
(5)

By setting $\dot{A}(t), \dot{I}(t), \dot{R}(t)$ to 0, we see that one equilibrium state of system (5) is given by $(A^e, I^e, R^e) = (0, 0, 0)$ with $S^e = 1$. This is the disease-free equlibrium (DFE) in the case of non-permanent immunity. Linearizing system (5) around (A^e, I^e, R^e) , we obtain the system Jacobian matrix,

$$J^{e} = \begin{bmatrix} q\beta - \kappa - \sigma & q\beta & 0\\ (1 - q)\beta + \sigma & (1 - q)\beta - \gamma & 0\\ \kappa & \gamma & -\delta \end{bmatrix}.$$
 (6)

This system will be globally asymptotically stable (GAS) around the DFE if all eigenvalues of J^e have negative real parts, as per Theorem 4.7 from [29]. Computing the characteristic polynomial for J^e , and applying the Routh-Hurwitz criterion gives the following.

Proposition 1: For the system given by (5), the DFE $(S^e, A^e, I^e, R^e) = (1,0,0,0)$ is GAS when

$$R_0 := \max\left(\frac{\beta}{\kappa + \gamma + \sigma}, \frac{\beta(q\gamma + (1 - q)\kappa + \sigma)}{\gamma(\kappa + \sigma)}\right) < 1. \quad (7)$$

Further, in the case where $\delta = 0$, that is when immunity following recovery from infection is permanent, the DFE will be any points $(S^e, A^e, I^e, R^e) = (c_S, 0, 0, c_R)$, where constants c_R, c_S satisfy $c_S + c_R = 1$. Analyzing the Jacobian for (5) in this case gives us that the equilibria $(S^e, A^e, I^e, R^e) = (c_S, 0, 0, c_R)$ are GAS again when (7) is satisfied. That is, this reproduction number expression provides an appropriate threshold for determining when the spread process for the SAIR(S) model will or will not spread exponentially in either of the scenarios of permanent or non-permanent immunity.

We further consider the case where the asymptomaticand symptomatic-infected individuals have different infection transmission rates. In the case of COVID-19, this difference could be partly due to the inability to conduct large-scale population testing in order to identify and isolate asymptomatic individuals. We denote the infection transmission rates for in-person contact from the two groups, resp., as β_A , β_I . Similar to the analysis above, we obtain the DFE at $(S^e, A^e, I^e, R^e) = (1,0,0,0)$ and the corresponding Jacobian,

$$J^{e} = \begin{bmatrix} q\beta_{A} - \kappa - \sigma & q\beta_{I} & 0\\ (1 - q)\beta_{A} + \sigma & (1 - q)\beta_{I} - \gamma & 0\\ \kappa & \gamma & -\delta \end{bmatrix}. \tag{8}$$

Following a similar approach as before yields:

$$R_0 := \max\left(\frac{q\beta_A + (1-q)\beta_I}{\kappa + \gamma + \sigma}, \frac{q\beta_A\gamma + \beta_I((1-q)\kappa + \sigma)}{\gamma(\kappa + \sigma)}\right)$$
(9)

For GAS, again it is required that $R_0 < 1$. We further compute the endemic equilibrium for (5), assuming non-permanent immunity, that is, $\delta > 0$. Setting $\dot{A}(t), \dot{I}(t), \dot{R}(t)$ to 0, we obtain the endemic equilibrium,

$$\begin{bmatrix} S^{e} \\ A^{e} \\ I^{e} \\ R^{e} \end{bmatrix} = \begin{bmatrix} \frac{\gamma(\kappa+\sigma)}{\beta(q\gamma+(1-q)\kappa+\sigma)} \\ \frac{q\delta\gamma\left(\beta(q\gamma+(1-q)\kappa+\sigma)-\gamma(\kappa+\sigma)\right)}{\beta(q\gamma+(1-q)\kappa+\sigma)\left(\gamma(\kappa+\sigma)+\delta(q\gamma+(1-q)\kappa+\sigma)\right)} \\ \frac{\delta((1-q)\kappa+\sigma)\left(\beta(q\gamma+(1-q)\kappa+\sigma)-\gamma(\kappa+\sigma)\right)}{\beta(q\gamma+(1-q)\kappa+\sigma)\left(\gamma(\kappa+\sigma)+\delta(q\gamma+(1-q)\kappa+\sigma)\right)} \\ \frac{\gamma(\kappa+\sigma)\left(\beta(q\gamma+(1-q)\kappa+\sigma)-\gamma(\kappa+\sigma)\right)}{\beta(q\gamma+(1-q)\kappa+\sigma)\left(\gamma(\kappa+\sigma)+\delta(q\gamma+(1-q)\kappa+\sigma)\right)} \end{bmatrix}$$
(10)

A complete analysis of this equilibrium is given in a longer version of this paper [30].

2) Networked Model N-SAIR(S):

We first consider the case with permanent immunity, implying $\delta = 0$. Given $s_i(t) = 1 - a_i(t) - p_i(t) - r_i(t)$ for all $t \ge 0, i \in [n]$, system (4) can be represented in matrix form as:

$$\begin{array}{lcl} \dot{a}(t) & = & [q(I-A(t)-P(t)-R(t))BW-\Sigma-K]a(t) \\ & + [q(I-A(t)-P(t)-R(t))BW]p(t) \\ \dot{p}(t) & = & [(1-q)(I-A(t)-P(t)-R(t))BW+\Sigma]a(t) \\ & + [(1-q)(I-A(t)-P(t)-R(t))BW-\Gamma]p(t) \\ \dot{r}(t) & = & Ka(t)+\Gamma p(t) \end{array}. \tag{11}$$

Here,

$$a(t) = \begin{bmatrix} a_1(t) \\ \vdots \\ a_n(t) \end{bmatrix}, p(t) = \begin{bmatrix} p_1(t) \\ \vdots \\ p_n(t) \end{bmatrix}, r(t) = \begin{bmatrix} r_1(t) \\ \vdots \\ r_n(t) \end{bmatrix},$$

with $n \times n$ matrices $A(t) = diag(a_i(t)), P(t) = diag(p_i(t)), R(t) = diag(r_i(t)), B = diag(\beta_i), K = diag(\kappa_i), \Gamma = diag(\gamma_i), \Sigma = diag(\sigma_i), \Delta = diag(\delta_i),$ and adjacency matrix W.

Setting $\dot{a}(t), \dot{p}(t), \dot{r}(t)$ to 0, we can compute the equilibrium state where $a^e = p^e = \vec{0}, r^e = \vec{r_c}$, where $\vec{r_c}$ is any nonnegative constant vector with elements $r_{c_i} < 1$. Linearizing the system (11) at the equilibrium (a^e, p^e, r^e) , we obtain the $3n \times 3n$ system Jacobian Matrix given by

$$J^{e} = \begin{bmatrix} q(I - R_{c})BW - \Sigma - K & q(I - R_{c})BW & 0\\ (1 - q)(I - R_{c})BW + \sigma & (1 - q)(I - R_{c})BW - \Gamma & 0\\ K & \Gamma & -\Delta \end{bmatrix}. (12)$$

Analysis of this Jacobian matrix leads to a set of constraints on the spectrum of the weighting matrix W. An alternative approach is to consider a Lyapunov stability analysis approach. Using a standard quadratic Lyapunov functional in the a(t) and p(t) vectors leads to the following sufficient condition for stability of the DFE:

$$\begin{bmatrix} qW & \frac{1}{2}W \\ \frac{1}{2}W & (1-q)W \end{bmatrix} \prec \begin{bmatrix} B^{-1}(\Sigma+K) & -\frac{1}{2}B^{-1}\Sigma \\ -\frac{1}{2}B^{-1}\Sigma & B^{-1}\Gamma \end{bmatrix}, \quad (13)$$

where \prec denotes relative definiteness of the matrices. That is, (13) provides a test that bounds the maximum eigenvalue of the *q*-scaled adjacency matrix W in terms of the minimum eigenvalue of a matrix consisting of block diagonal entries of ratios of healing and transition rates $(\kappa_i, \gamma_i \text{ and } \sigma_i)$ to infection rates (β_i) ; this loosely generalizes the usual R_0 threshold.

III. SIMULATIONS

We first simulate a baseline model for (4), for which we assume homogeneous spread parameters and a five-subpopulation network structure. We assume the total population size is 10,000 and the respective subpopulations denoted U, V, X, Y, and Z have populations 2000,2500,1500,3500, and 500, resp.. We assume the cities are fully connected with uniformly distributed edge weights, thus this baseline model is equivalent to a single group model. We use the estimation results from local data (discussed in IV) in addition to drawing on the literature (e.g.,[31] [32]) to inform our parameter value selection: $(q,\beta,\sigma,\gamma,\kappa,\delta)=(0.7,0.25,0.15,0.11,0.08,0.0001)$. We set the initial proportions of the A,I,R compartments as

$$\begin{split} a(0) &= (a_U(0), a_V(0), a_X(0), a_Y(0), a_Z(0)) \\ &= (0.006, 0.004, 0.012, 0.004, 0.004) \\ p(0) &= (p_U(0), p_V(0), p_X(0), p_Y(0), p_Z(0)) \\ &= (0.005, 0.002, 0.008, 0.003, 0.002) \\ r(0) &= (r_U(0), r_V(0), r_X(0), r_Y(0), r_Z(0)) \\ &= (0.007, 0.003, 0.010, 0.008, 0.005). \end{split}$$

Simulating the SAIRS model over 60 days results in the disease progression shown in Fig.1. Note that peak active

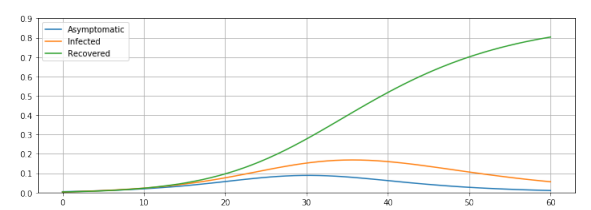


Fig. 1: Group/Network SAIRS Simulation: Baseline Model infection occurs on day 33, that is p(t) + a(t) attains a maximum of approx. 28% on day t = 33. By day 60, approx. 87% of the entire population has been or is infected; assuming a mortality rate of 4%, that would correspond to 348 deaths in the two month time span. Again we note this model assumes homogeneous mixing within the entire population with no mitigation policies enacted.

A. Asymptomatic Effects

One obstacle in the control of COVID-19 is the challenge of identifying and monitoring individuals in the asymptomatic-infected subgroup. Herein we explore the impact of this subgroup on the epidemic. We first assume there are no control policies imposed on either the asymptomatic or symptomatic infected subgroups. We use the group model (3) with parameters as given previously, which results in a basic reproduction number $R_0 \approx 2.5$ using (7). We then impose different isolation policies on the asymptomatic and symptomatic (A and I) subgroups, which we implement by changing the respective effective transmission rate. We consider the resulting effective R_0 (denoted by R), peak infection levels (Peak Infection) and the corresponding day of peaks (Peak Day), and the percentage of population that is or has been infected by Day 80 (%-AIR) as measures for the extent of the epidemic spread. By setting initial proportions for the A, I, R compartments for each subpopulation as (A(0), I(0), R(0)) = (0.004, 0.002, 0.003), we obtained simulation results as shown in the table below.

Simulation results: Varying isolation policies on A and I

Isolation	β_A	β_I	R	Peak In-	Peak	%-AIR
Level				fection	Day	
No isolation	0.25	0.25	2.5	25%	35	87%
on A or I						
Moderate iso-	0.25	0.11	1.5	9%	60	49%
lation on I, no						
isolation on A						
Strict isola-	0.25	0.06	1.2	2.5%	75	17%
tion on I, no						
isolation A						
Moderate iso-	0.11	0.11	1.09	1%	87	7.7%
lation A and I						
Strict isola-	0.0125	0.0125	0.89	0.5%	4	1%
tion A and I						

We note that with isolation measures on only the I subgroup, the epidemic progresses more slowly and mildly. With moderate and strict isolation policies in effect on the I subgroup, and with a population base of 10000 and a mortality rate of 4%, approx. 152 and 280, resp., fewer deaths occur over the 80 days than with no isolation. In the scenario where asymptomatic individuals are also identified and isolated, under both moderate and stringent policies, the spread is mitigated by a significant amount.

In particular, with only moderate isolation on both the *A* and *I* subgroups (Fig.2), the epidemic is controlled within three months. At a 4% mortality rate, approx. 37 fewer deaths occur as compared to applying stringent control policies on only the *I* group.

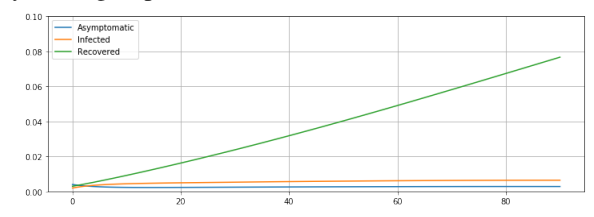


Fig. 2: Moderate isolation of both Symptomatic and Asymptomatic Infected subgroups

An additional measure to consider is the effective reproduction number under the different isolation policies. Moderate isolation of both A and I subgroups gives $R \approx 1.09$, while stringent isolation on just the I subgroup gives $R \approx 1.2$. These results confirm the expected, that identification and isolation of both the asymptomatic and symptomatic infected individuals is more effective in curbing the spread of the epidemic than identification and isolation of only the symptomatic subgroup.

B. Network Effects

We now consider the effects that a more realistic interaction structure has on epidemic spread over a population. We consider the 5-node network introduced earlier, and consider the removal of some edges between nodes. We first consider an interconnection network structure with adjacency matrix

$$W = \begin{bmatrix} \frac{1}{3} & \frac{1}{3} & \frac{1}{3} & 0 & 0\\ \frac{1}{3} & \frac{1}{3} & 0 & 0 & \frac{1}{3}\\ \frac{1}{3} & 0 & \frac{1}{3} & \frac{1}{3} & 0\\ 0 & 0 & \frac{1}{2} & \frac{1}{2} & 0\\ 0 & \frac{1}{2} & 0 & 0 & \frac{1}{2} \end{bmatrix}.$$
 (14)

Using the same parameters and initial conditions as in the baseline model, simulations show that, with a less strongly connected network, the epidemic spreads more slowly and weakly. Among the total five cities, subpopulation X experiences most rapid spread: a peak infection level of 21% occurs at day 37; by day 60, approx. 87% of city X population is or has been infected. However, in total, approx. 480 fewer individuals over the five cities are infected as compared to the fully connected (i.e., complete) baseline model.

To explore the impact of quarantines and stronger social distancing measures, we consider a population further divided into 50 smaller subpopulations, and generate a stochastic adjacency matrix with each node only connected to 20 other randomly selected nodes out of the 50 possible. Initial conditions a(0), p(0), r(0) are chosen randomly using $a_i(0) \sim \mathcal{N}(0.04, 0.005), \ p_i(0) \sim \mathcal{N}(0.02, 0.005), \ r_i(0) \sim$ $\mathcal{N}(0.03, 0.005)$, but restricting all values to be non-negative. Simulations for 3 of the 50 sub-populations (selected randomly) are shown in Fig.3. Under this more extensive isolation scenario, the epidemic decays much faster than under the previous strongly connected network. Subpopulations 4, 22 and 34, resp., reach their peak infection levels at days 21, 59 and day 0. Among the three subpopulations, subpopulation 22 is the most highly infected group. However, overall after 60 days, approx. only 13.6% of the population has been or is infected, which is a reduction of 73.4% of the population compared to the fully connected network (Fig.1), and a reduction of 67.7% compared to the strongly connected network. These simulations again demonstrate the expected, that social distancing measures such as quarantining within small communities or family units controls the spread of the epidemic, as has been seen in practice in many communities. From the perspective of the group model, extensive isolation policies help reduce transmission rates for person-to-person contact, which results in both faster flattening of the infection curve and fewer infected individuals (asymptomatic and symptomatic) in the whole population.

IV. PARAMETER ESTIMATION

In this section we briefly discuss results from a simple least-squares approach for parameter estimation for the discrete-time N-SAIRS model given in (15) as applied to local COVID-19 data.

As our data results from sampling on a daily basis, a discrete-time model is better suited for estimating and evaluating model parameters. Applying a forward Euler's method to the continuous-time networked system (4), gives us the discrete-time networked SAIRS model,

$$a_{i}^{k+1} = a_{i}^{k} + q\beta_{i}(1 - a_{j}^{k} - p_{j}^{k} - r_{j}^{k})\sum_{j}W_{ij}(a_{j}^{k} + p_{j}^{k}) - \sigma_{i}a_{i}^{k} - \kappa_{i}a_{i}^{k}$$

$$p_{i}^{k+1} = p_{i}^{k} + (1 - q)\beta_{i}(1 - a_{j}^{k} - p_{j}^{k} - r_{j}^{k})\sum_{j}W_{ij}(a_{j}^{k} + p_{j}^{k}) + \sigma_{i}a_{i}^{k} - \gamma_{i}p_{i}^{k}$$

$$r_{i}^{k+1} = r_{i}^{k} + \kappa_{i}a_{i}^{k} + \gamma_{i}p_{i}^{k} - \delta_{i}p_{i}^{k}.$$
(15)

Since our simulation update will be daily and the sampling rate is once-per-day, the sampling parameter will be 1 and thus is not explictly noted above.

A. Asymptomatic Proportion Estimation

Due to the difficulties in identifying and monitoring infected individuals without symptoms, explicit and unbiased

inf. for asymptomatic-infected estimations is not always available. Applying the Next-Day Law approach proposed by Nesterov in [33], we estimate asymptomatic numbers per day, based on a latent period assumption, and use these to estimate a proportion q of the asymptomatic subpopulation as a fraction of the total population. We note that this approach more accurately gives us a pre-symptomatic subpopulation proportion. From these estimated daily asymptomatic counts, we are able to estimate the proportions q and 1-q of asymptomatic and symptomatic-infected subgroups. Using the first two expressions in (15), we have

$$\frac{a_i^{k+1} - a_i^k}{p_i^{k+1} - p_i^k} \approx \frac{q}{1 - q}.$$

Hence, we can simply estimate q by $\frac{a_i^{k+1}-a_i^k}{(a_i^{k+1}-a_i^k)+(p_i^{k+1}-p_i^k)}$.

B. Least squares estimation of model parameters

With q known (or estimated), we can apply the least-squares estimation approach first outlined in [34], and described explicitly for SAIRS models in [26] to estimate the model parameters β_i , σ_i , κ_i , γ_i , and δ_i .

We consider local COVID-19 testing-site data from Champaign County, Illinois, dating from April to August, 2020, to compute parameter estimations for different phases of the state restore plans, scheduled as:

Phase 1 : *Rapid Spread* (04/01/2020 – 05/01/2020)

Phase 2: Flattening (05/01/2020 - 05/29/2020)

Phase 3 : *Recovery* (05/29/2020 – 06/26/2020)

Phase 4 : *Revitalization* (06/26/2020 – 09/26/2020)

We assume a latent period of $\Delta = 6$ days, resulting in the parameter estimates shown in the table below:

Phases	q	β	σ	γ	κ	R_0
Phase 2	0.7	0.06	0.22	0.15	-0.10	1.004
Phase 3	0.6	0.07	0.15	0.15	-0.05	1.156
Phase 4	0.6	0.07	0.08	0.11	0.02	1.104

We note that, as the epidemic progresses, the basic reproduction number R_0 first rises, and then decreases with the implementation of consistent quarantine and other social distancing measures.

These preliminary results expose issues with real data based estimation and analysis. For example, due to the reduced availability of tests and test-sites in the early stages of the epidemic, as well as non-random samples, the testing population presented in the data is skewed by the symptomatic individuals. This hinders accurately capturing the true proportion of the asymptomatic subgroup, as well as an accurate prevalence rate of infection in the total population. In addition, our assumption of a constant latent period is not consistent with the nature of COVID-19; the latent period value we have used is an average value [31], [32]. These issues lead to estimation errors, such as the negative recovery rate values for κ in Phase 1 and Phase 2.

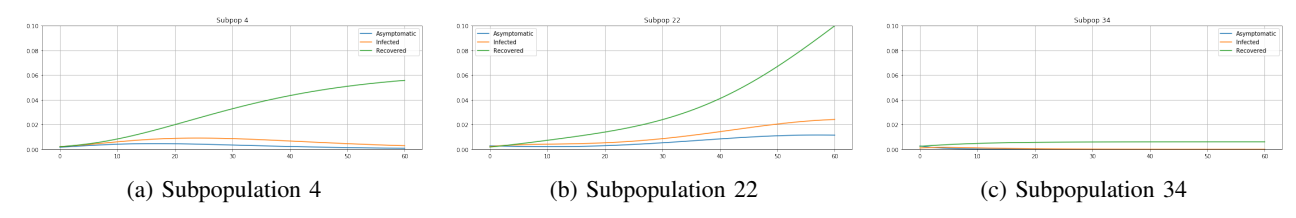


Fig. 3: Weakly Connected Network Simulation Results

V. FUTURE WORK

Our ongoing efforts include pursuing approaches for model parameter estimation under non-random and missingsample data sets, and investigating Bayesian statistical approaches for estimating true prevalence of epidemics under biased information.

ACKNOWLEDGMENTS

The authors would like to thank Sam Dekhterman for data collection, and Dr. Joseph Kim, M.D., Ph.D., for many useful and interesting discussions, and for providing informative references. This work has been supported in part by Jump-ARCHES endowment through the Health Center for Engineering Systems Center at the University of Illinois, Urbana-Champaign, the C3.ai Digital Transformation Institute, and the NSF grant ECCS-2032321.

REFERENCES

- [1] D. Bernoulli, "Essai d'une nouvelle analyse de la mortalité causée par la petite vérole et des avantages de l'inoculation pour la prévenir," Histoire de l'Acad. Roy. Sci. avec Mém. des Math. et Phys. and Mém, pp. 1-45, 1760.
- [2] W. O. Kermack and A. G. McKendrick, "Contributions to the mathematical theory of epidemics. II. The problem of endemicity," Proc. of the Royal Society A, vol. 138, no. 834, pp. 55-83, 1932.
- [3] S. Scarpino and G. Petri, "On the predictability of infectious disease outbreaks," Nature Comm., vol. 10, 2019.
- [4] S. Funk, E. Gilad, C. Watkins, and V. A. A. Jansen, "The spread of awareness and its impact on epidemic outbreaks," Proc. of The National Academy of Sciences, vol. 106, pp. 6872-6877, 2009.
- [5] C. Granell, S. Gómez, and A. Arenas, "Dynamical interplay between awareness and epidemic spreading in multiplex networks," Phys. Rev. Lett., vol. 111, p. 128701, Sep 2013. [Online]. Available: http://link.aps.org/doi/10.1103/PhysRevLett.111.128701
- [6] K. Paarporn, C. Eksin, J. S. Weitz, and J. S. Shamma, "Networked SIS epidemics with awareness," IEEE Trans. Computational Social Systems, vol. 4, no. 3, pp. 93-103, 2017.
- [7] J. Liu, P. E. Paré, A. Nedić, C. L. Beck, and T. Başar, "On a continuous-time multi-group bi-virus model with human awareness," in Proceedings of The IEEE Conf. on Decision and Control, Dec 2017, pp. 4124-4129.
- [8] S. Xu, W. Lu, and Z. Zhan, "A stochastic model of multivirus dynamics," IEEE Trans. on Dependable and Secure Computing, vol. 9, no. 1, pp. 30-45, 2012.
- [9] P. E. Paré, J. Liu, C. L. Beck, A. Nedić, and T. Başar, "Multicompetitive viruses over static and time-varying networks," in Proc. of American Control Conference, 2017, pp. 1685-1690.
- [10] P. E. Pare, J. Liu, C. L. Beck, A. Nedić, and T. Basar, "Multicompetitive viruses over time-varying networks with mutations and human awareness," Automatica, 2020, accepted.
- [11] J. O. Kephart and S. R. White, "Directed-graph epidemiological models of computer viruses," in IEEE Symposium on Security and Privacy, 1991, pp. 343-361.
- [12] A. Ganesh, L. Massouli, and D. Towsley, "The effect of network topology on the spread of epidemics," in 24th Annual Joint Conference of the IEEE Computer and Communications Societies, vol. 2, 2005, pp. 1455-1466.
- [13] M. Draief and L. Massoulie', Epidemics and rumours in complex networks. Cambridge University Press, 2010.

- [14] R. Pastor-Satorras, C. Castellano, P. Van Mieghem, and A. Vespignani, "Epidemic processes in complex networks," Reviews of Modern Physics, vol. 87, no. 3, p. 925, 2015.
- C. Nowzari, V. M. Preciado, and G. J. Pappas, "Analysis and control of epidemics: A survey of spreading processes on complex networks," IEEE Control Systems Magazine, no. 1, pp. 26-46, 2016.
- [16] W. Feller, "On the integro-differential equations of purely discontinuous markoff processes," Trans. of the American Mathematical Society, vol. 48, no. 3, pp. 488–515, 1940. [17] T. G. Kurtz, "The central limit theorem for Markov chains," *The*
- Annals of Probability, vol. 9, no. 4, pp. 557-560, 1981.
- [18] P. V. Mieghem, J. Omic, and R. Kooij, "Virus spread in networks," IEEE/ACM Trans. on Networking, no. 1, pp. 62-68, 2009.
- [19] S. Chatterjee and R. Durrett, "Contact processes on random graphs with power law degree distributions have critical value 0," The Annals of Probability, no. 6, pp. 2332-2356, 2009.
- [20] A. Fall, A. Iggidr, G. Sallet, and J. J. Tewa, "Epidemiological models and Lyapunov functions," Mathematical Modelling of Natural Phenomena, vol. 2, no. 1, pp. 62-83, 2007.
- [21] P. E. Paré, C. L. Beck, and A. Nedić, "Epidemic processes over timevarying networks," IEEE Trans. on Control over Network Systems, no. 3, pp. 1322-1334, 2018.
- [22] H. J. Ahn and B. Hassibi, "Global dynamics of epidemic spread over complex networks," in Proceedings of the IEEE Conference on Decision and Control, 2013, pp. 4579-4585.
- [23] Y. Wang, D. Chakrabarti, C. Wang, and C. Faloutsos, "Epidemic spreading in real networks: an eigenvalue viewpoint," in Proc. of the 22nd International Symposium on Reliable Distributed Systems, 2003, pp. 25-34.
- [24] C. L. Beck, "Accounting for network structure and dynamics in epidemic models," in Health Care Engineering Systems Center UIUC, COVID-19 Virtual Summit, 2020, April.
- [25] C. L. Beck, "Epidemic processes and network structure," in First Call to Arms Workshop, NSF NeTs Community and the Ohio State University, 2020, April.
- [26] P. Pare, C. Beck, and T. Başar, "Modeling, estimation, and analysis of epidemics over networks: An overview," Annual Reviews in Control, 2020, accepted.
- [27] M. Grunnill, "An exploration of the role of asymptomatic infections in the epidemiology of dengue viruses through susceptible, asymptomatic, infected and recovered (SAIR) models," Journal of Theoretical Biology, vol. 439, pp. 195-204, 2018.
- B. W. L. Zhu, "Stability analysis of a sair rumor spreading model with control strategies in online social networks," Information Science, vol. 526, 2020.
- [29] H. K. Khalil, Nonlinear Systems. Prentice Hall, 2002.
 [30] X. Bi and C. L. Beck, "On the role of asymptomatic carriers in epidemic spread processes," Preprint, 2021, https://arxiv.org/pdf/2103.11411.pdf.
- S. A. Lauer, K. H. Grantz, Q. Bi, M. Q. Z. F. K. Jones, H. R. Meredith, A. S. Azman, N. G. Reich, and J. Lessler, "The incubation period of coronavirus disease 2019 (covid-19) from publicly reported confirmed cases: Estimation and application," *Annals of Internal Medicine*, 2020. [Online]. Available: https://www.acpjournals.org/doi/10.7326/M20-0504
- D. P. Oran and M. E. J. Topol, "Prevalence of asymptomatic sars-cov-2 infection; a narrative review," Annals of Internal Medicine, 2020. [Online]. Available: https://www.acpjournals.org/doi/10.7326/M20-3012
- [33] Y. Nesterov, "Online prediction of covid19 dynamics.belgian case study," Preprint, 2020, https://arxiv.org/pdf/2007.11429.pdf.
- P. E. Paré, J. Liu, C. L. Beck, B. E. Kirwan, and T. Başar, "Analysis, identification, and validation of discrete-time epidemic processes,' IEEE Trans. on Control Systems Technology, vol. 28, no. 1, pp. 79-93,